Nano Energy 80 (2021) 105519

Contents lists available at ScienceDirect

Nano Energy

journal homepage: http://www.elsevier.com/locate/nanoen

Full paper

PANI/PVDF-TrFE porous aerogel bulk piezoelectric and triboelectric hybrid nanogenerator based on in-situ doping and liquid nitrogen quenching

Shengrui Yu [a,1], Yongkang Zhang [a,1], Zhaohan Yu [b,1], Jiaqi Zheng [b], Yunming Wang [b,*], Huamin Zhou [b,*]

[a] School of Mechanical and Electronic Engineering, Jingdezhen Ceramic Institute, Jingdezhen 333403, PR China
[b] School of Materials Science and Engineering, Huazhong University of Science & Technology, Wuhan 430074, PR China

ARTICLE INFO

Keywords:
Bulk nanogenerator
In-situ doping
Generated β-PVDF-TrFE
Liquid nitrogen quenching
Piezo-triboelectric

ABSTRACT

Limited by the inherent properties of being difficult to be polarized due to its high resistance, PVDF bulk material with high β-phase content is hard to obtain by conventional methods which are suitable for membrane material. Herein, a novel strategy is proposed for the mass production of high-performance β-PVDF-based piezoelectric and triboelectric hybrid nanogenerator (PTNG) employing large-scale PVDF films or bulks by using liquid nitrogen to induce a phase transition and in-situ doped conductive polyaniline (PANI). Polyvinylidene fluoride-trifluoroethylene (PVDF-TrFE) with high piezoelectric coefficient, filled with PANI as a conductive material and sodium carboxymethyl cellulose (SCMC) for increasing porosity, is hot pressed to obtain a composite piezoelectric polymer for PTNG. The subsequent "quenching" process of the piezoelectric polymer allows its high content of β-phase, which in turn makes the PTNG exhibit excellent piezoelectric properties. The optimal output of the PTNG, with a β-phase content of up to 71%, reaches 246 V and 122 μA at the frequency of 30 Hz and pressure of 0.31 MPa, and the power density is calculated to be 6.69 W/m^2. Moreover, the PTNG can directly light up 119 blue light-emitting diodes (LEDs) with a size of 3 mm in series. The excellent performance verifies the reliability and accuracy of the method, that is, the β-phase transformation of disordered amorphous PVDF occurs at low temperature and high-rate quenching, and PANI opens the channel for carriers to move charge in the bulk material. This innovative method presented here is a simple and efficient approach for preparation of bulks with high β-phase and low internal resistance, which undoubtedly provides a feasible direction for the industrialization of high-performance PENGs.

1. Introduction

β-phase polyvinylidene fluoride (β-PVDF), exhibiting extraordinary piezoelectric property [1], flexibility [2] as well as high durability [3], has been extensively applied as piezoelectric polymer material in self-powered sensor devices such as rail transit [4] (e.g. pressure sensors [5], speed sensors [6] and vibration sensors [7]), medical health [8] (e.g. pacemakers [9] and pulse sensors [10]) and artificial intelligence [11] (e.g. portable devices [12,13] and electronic skin [14,15]). However, untreated PVDF usually crystallizes in non-polar α-phase with negligible piezoelectricity [16]. For the transformation from α-phase to β-phase with high piezoelectric coefficient [17], several methods have been explored including electric field polarization [18] and mechanical stretching [19–22]. Limited by the large internal resistance and the low-dimensional characteristics [23,24] of the piezoelectric material, the large-scale phase transition of PVDF bulk materials suitable for high energy storage and components cannot be realized by conventional methods. Therefore, it is an urgent demand for a low-cost, high-efficiency method to achieve phase transition induction of large-size films or even bulk materials.

As a traditional craft of heat treatment, "quenching" may be an ideal approach to conquer these problems, which means heating the PVDF bulk at a certain temperature, and then rapidly cooling the polymer to crystallize the polymer and induce β-PVDF [25]. Compared with room temperature water bath and ice water bath, liquid nitrogen has the characteristics of ultra-low temperature, which can achieve a higher cooling rate and easily form uniform β-phases [26]. In addition, using PVDF copolymer [27,28], adding functional fillers [10,29,30] for

* Corresponding authors.
E-mail address: wang653@hust.edu.cn (Y. Wang).
[1] These three authors made an equal contribution to this work.

https://doi.org/10.1016/j.nanoen.2020.105519
Received 13 August 2020; Received in revised form 1 October 2020; Accepted 17 October 2020
Available online 27 October 2020

modification, improving the porosity of materials [31–33] and optimizing structural design [34–36] also have a significant enhancement on the performance of nanogenerators (NGs). Polyvinylidene fluoride-trifluoroethylene (PVDF-TrFE) copolymers are more likely to exhibit all trans structure because of the larger steric hindrance of fluorine atoms in TrFE monomers which are connected with hydrogen atoms on the same carbon atom, showing greater dielectric response and electroactive properties compared with PVDF [1,37]. Though the above methods have significant enhancement, it is noted that the appropriate preparation methods of porous materials [31] and the selection of fillers [38] are particularly important for the preparation of high-performance nano-generator devices.

To meet these challenges, we proposed a novel strategy to prepare large-scale polyaniline/PVDF-TrFE (PANI/PVDF-TrFE) porous aerogel bulk piezoelectric/triboelectric nanogenerator (PTNG) based on in-situ doping and liquid nitrogen quenching. The composite aerogel, prepared by freeze-drying method with PVDF-TrFE copolymer as the main substrate, sodium carboxymethyl cellulose (SCMC) as thickener [39] and PANI as conductive filler [40,41], induce β-phase by rapid cooling of liquid nitrogen after thermoforming. On this basis, the effects of β-phase conversion, PANI filling rate, porosity and thickness on the electrical properties of PANI/PVDF-TrFE piezoelectric bulks were studied. The optimal performance of the PANI/PVDF-TrFE PTNG can reach an output voltage of 246 V, a short-circuit current of 122 μA, a power density of 6.69 W/m^2 and can light up 119 blue light-emitting diodes in series with a size of 3 mm. Compared with traditional methods, the PANI/PVDF-TrFE porous aerogel bulk fabricated by the novel strategy can be directly used without subsequent electric field polarization, and its β-phase content is as high as 71%, which has less energy consumption and shorter preparation period. Our work solves the problem of polarization of PVDF bulk, taking a big step forward towards PVDF-based NGs' three-dimensional manufacturing and further practical applications.

2. Experimental section

2.1. Preparation of porous PANI/PVDF aerogel bulk

The preparation of PANI/PVDF-TrFE aerogel bulks is mainly divided into two stages: first, the mixed solution is prepared by the ultrasonic stirring and freeze-drying method to acquire composite aerogel materials; second, the aerogel bulk is obtained by hot pressing and then rapidly cooled in liquid nitrogen to achieve an effective phase transformation. The specific steps for preparing the PANI/PVDF-TrFE aerogel bulk are illustrated in Fig. 1: (1) SCMC (Sinopharm Chemical Reagent Co., Ltd., China) was dissolved in hydrochloric acid (HCl), and then the ultrasonic-prepared PVDF-TrFE (70:30 mol%) emulsion and the PANI (Wuhan Yuancheng Gongchuang Technology Co., Ltd., China) dispersion were added successively under mechanical stirring to prepare the homogeneous solution. The pH was adjusted by NaOH solution. Particularly, sodium dodecyl sulfate (SDS, Aladdin Reagent Co., Ltd., China) was used as a surfactant to promote the dispersion of PVDF-TrFE and PANI dispersion was obtained by ultrasound in HCl solution. (2) To avoid solute deposition, the solution was cooled rapidly in the ethanol-liquid nitrogen to prepare the frozen body. The low temperature viscosity of ethanol-liquid nitrogen can help control the balance of freezing body, which contributes to the unidirectional growth of ice crystals from the bottom up [42]. (3) Freeze-drying the frozen body for 3 days to prepare a porous composite aerogel. (4) The aerogel was then pressured at 4 MPa and 220 °C for 1 h into a PANI/PVDF-TrFE bulk. (5) Place the pressed bulk parallel to the surface of liquid nitrogen to realize rapid quenching. (6) The bulk was finally immersed in water followed by ultrasonic repeatedly to completely remove internal impurities and reduce internal stress.

2.2. Assembly of PANI/PVDF-TrFE piezoelectric and triboelectric hybrid nanogenerator

The PANI/PVDF-TrFE bulks with different thicknesses (0.12–0.33 mm) were dried at room temperature, cut into 1 cm × 2 cm rectangles, and then directly assembled into PTNGs with the condition of external copper foil.

2.3. Measurement of the PTNG

The output performance of PANI/PVDF-TrFE PTNG was tested using an oscillation excitation system. The measurement platform is composed of an excitation system and a signal sampling system, which can simulate the vibration of the actual environment and collect the output signals respectively. The excitation system consists of a vibration exciter (DH 40050, Donghua Test Technology Co., Ltd., China), a power amplifier (DH 5871, Donghua Test Technology Co., Ltd., China), and a signal generator (DH 1301, Donghua Test Technology Co., Ltd., China). A pressure sensor (PCB PIEZOTRONICS, 208C02) and a PXI system (Quad-core embed controller, NI PXIe-8135; Chassis, NI PXIe-1082; Acquisition card, NI PXIe-4499, National Instruments, US) are used to measure the pressure exerted on the device. The signal generator generates frequency and voltage signals. The power amplifier increases the voltage signal and drives the exciter to work. Signal sampling systems include oscilloscopes (TBS 1102, Tektronix, US) and bass noise amplifiers (A Stanford Research SR570), which sample the output voltage and current respectively. The relevant parameters and diagram of the test

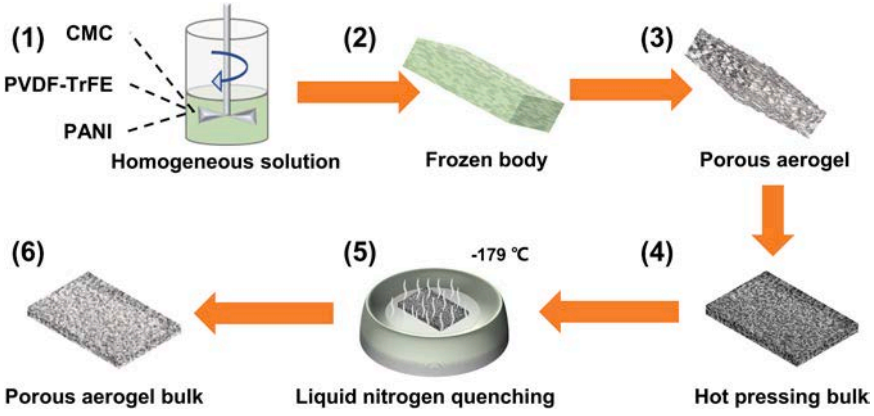

Fig. 1. Schematic diagram of the preparation process of porous PANI/PVDF-TrFE aerogel bulk.

are shown in Table S1 and Fig. S1.

2.4. Characterization

Field emission scanning electron microscope (JSM-7600F, JEOL Co., Ltd., Japan) and Brunner–Emmet–Teller (BET) were used to characterize the morphology of the samples. The bulk thickness was measured using a thickness gauge (033004, Development Co., Ltd., China). X-ray diffractometer (x′pert3 powder, PANalytical B.V., The Netherlands) and Fourier transform infrared (VERTEX 70 Bruker, Germany) were employed for phase analysis.

3. Results and discussion

A schematic diagram in Fig. 2a depicts the molecular morphological character during the dissolution of composite materials. SCMC, which initially existed in acidic aqueous solution in the form of micelles and free state [43], gradually adheres to the substrate of PVDF-TrFE after adding its dispersion due to hydrogen bonding. Subsequently, with the addition of conductive PANI, the polymer chains are entangled with each other under the action of strongly interacting hydrogen bonds and dipoles [44].

The high β-phase content and low resistance of the bulk play a significant role in improving the output performance of the self-powered components. The schematic diagram in Fig. 2b illustrates the phase transition process of the PANI/PVDF-TrFE bulk from α-phase to β-phase. The disordered molecules in the molten α-PVDF are transformed into an ordered arrangement of β-phase due to the rapid cooling of liquid nitrogen from the bottom up. Further, the PVDF-TrFE bulk is immersed in parallel to the surface of liquid nitrogen, rapidly cooled and recrystallized from bottom to top, thereby obtaining a highly uniformly oriented β-phase (Fig. 5). As shown in Fig. 2f and g, the optimal output properties of PTNG with voltage and current, which are 246 V and 122 μA, respectively.

In order to investigate the dominant mechanism of liquid nitrogen quenching in realizing the β-phase transformation of the bulk, the bulk

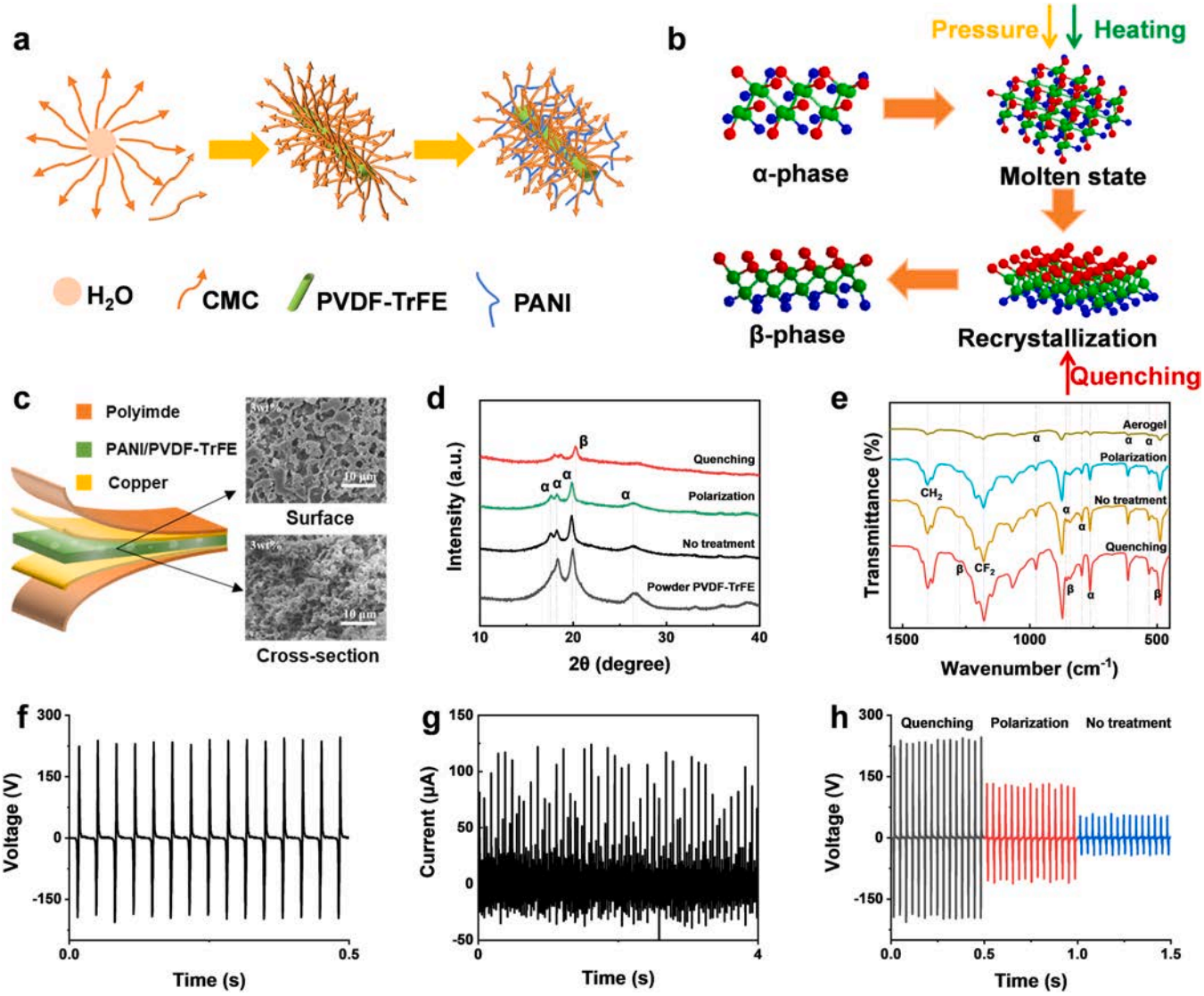

Fig. 2. (a) The possible interaction mechanism between SCMC, PANI and PVDF-TrFE chains, inducing the formation of a conductive network; (b) The phase transformation process of PVDF-TrFE under hot pressing and liquid nitrogen quenching; (c) Structure diagram of the PTNG and surface and cross-section SEM images of the aerogel bulk; (d) XRD pictures under different polarization conditions; (e) FTIR image of aerogel and quenched bulk; (f) The optimal output voltage and (g) current of the quenched PANI/PVDF-TrFE PTNG; (h) Output voltage of devices fabricated under different polarization conditions.

prepared by hot pressing is divided into three parts for post-treatment: liquid nitrogen quenching, high-voltage electric field polarization and no treatment, of which the latter two groups are control experiments. The XRD pattern of PVDF-TrFE powder has obvious diffraction peaks only at about 18.3°, 19.9° and 26.5°, which are determined as α-phase [25] (Fig. 2d). Quenching changed the intensity and position of the PVDF diffraction peak, and the α-phase diffraction peaks decreased or disappeared at 18.3° and 26.5°. The α-phase diffraction peak shifted to the left at 19.9°, forming a new diffraction peak of β-phase (110) (200) at 20.23°. Moreover, it should be noted that there was no obvious change in the phase of the bulk induced by the electric field of 2 kV/cm, which indirectly indicates the superiority of liquid nitrogen quenching in realizing the phase transformation of bulk materials.

The phase change and composition of the sample were further analyzed by FTIR. For the PANI powder samples, the absorption bands at 1562 and 1475 cm^{-1} (Fig. S2a) correspond to the stretching modes of quinone ring and benzene ring, respectively [45]. The characteristic bands of aromatic rings located at 1453 and 1607 cm^{-1} were observed in the composite products, which confirmed the existence of PANI [15]. The band of the framework stretching vibration of aromatic hydrocarbons (C=C) shifted its frequency from 1500 cm^{-1} to ~ 1510 cm^{-1} due to the action of the power supply group $-NH_2$. For the PVDF-TrFE, the bands at 871, 1180 and 1400 cm^{-1} correspond to the stretching vibration of C–F, the deformation vibrations and asymmetric stretching of C–H bond connected to $-CF_2$ in PVDF respectively [46], and changed significantly with the addition of SCMC and PANI in Fig. S2, which indicates that hydrogen bonds and strong dipole-dipole interactions may be formed between PVDF-TrFE, SCMC and PANI molecules. The bands of α-PVDF at 531, 614, 763, 795, 853 and 975 cm^{-1} were observed on the infrared spectrum of the aerogel [47]. After hot pressing and liquid nitrogen quenching, the stretching vibration characteristic bands within the cellulose backbone at 1112 and 1149 cm^{-1} disappeared, and showed bands regarded as β-PVDF at 510, 841 and 1276 cm^{-1}, which indicated the decomposition of SCMC [48] and verified the results of XRD analysis [49]. Meanwhile, the content of PVDF β-phase changed slightly with the content of PANI (Fig. S2c). Results of XRD and FTIR, indicate that the PVDF-TrFE doped with 3 wt% PANI achieved an extremely high phase transition through liquid nitrogen quenching, with a β-phase content reaching 71%.

To verify the effect of β-phase on the excellent electrical properties of PTNG, the output performance of the different post-treated samples under the oscillation excitation of 30 Hz and 0.31 MPa were compared. As shown in Fig. 2h, the quenched PTNG with 71% β-phase exhibits the optimal output of 246 V, while that of untreated and electric field polarization are only 58.2 V and 132 V, respectively. Untreated PTNG crystallized in nonpolar α-phase cannot exhibit piezoelectricity, and its output comes from the triboelectricity generated by the friction between the internal surfaces of its internal pores [50]. Electric field polarization can induce a certain amount of β-phase in PTNG to improve the piezoelectric performance, but the degree and effect of phase transition are much lower than that of quenching, which demonstrates the inadequate of traditional electric field polarization method and strongly verifies that the liquid nitrogen quenching has a vigorous applicability in the rapid and effective phase transition of bulk materials.

Compared with traditional PENGs, the prepared PANI/PVDF-TrFE porous bulk has a larger surface size (Fig. S3), which can be directly applied to PTNG by cutting, demonstrating the application potential of this method in large-scale manufacturing of piezoelectric materials. The scanning electron microscope image of sample presents a three-dimensional network structure composed of nanoscale flakes and shows numerous and interconnected pore structure on the surface and cross section of the aerogel bulk (Fig. 2c), which results from intrinsic character of aerogel material and decomposition of SCMC carbonization [51] during hot pressing and the removal of certain materials by ultrasonic cleaning. The existence and non-uniformity of the pore structure will limit the increase of the polarization intensity, and hardly realize the transformation of crystal form, which further confirms the superiority of quenching process in realizing phase transformation of porous bulk materials (Fig. 2d).

PTNG is a sandwich structure [52,53] composed of copper foil as an electrode and piezoelectric material, and its outer insulating layer is composed of a polyimide film, as shown in Figs. 2c and 3a. Freely mobile electrons in the conductive PANI (Fig. 3a) can promote the movement of charge in the material through the conductive network formed between PANI and PVDF-TrFE, improving the energy transfer efficiency. The deformation of the bulk under the periodic stresses of flapping will leads to the change of dipole moment, thereby generating piezoelectric charges [54]. Besides, due to the difference in curvature of the irregular pores [55] inside the bulk (Fig. 3c and d), the upper and lower surfaces of the pores can generate triboelectric charges during the contact-separate process caused by periodic flapping, resulting in higher charge density and potential [56,57]. As shown in Fig. 3b, in the initial state, the bulk does not generate any charge in the ideal state. Once the PANI/PVDF-TrFE bulk is deformed under positive stress, due to the synergistic effect of piezoelectricity and triboelectricity, positive and negative charges accumulate on the upper and lower surfaces of the bulk to generate a potential difference, which in turn promotes the flow of external circuit charges [28]. When the PTNG is released at the limit position, the potential gradually decreases due to the restoration of the layer and the separation of the friction surface, and the electrons return through the external circuit. Under such cyclic stress, PTNG generates alternating current and can achieve higher electrical output performance than general PENGs [58].

In order to detect the sensitivity of PTNG under actual stress, we simulated the actual working conditions of PTNG by changing the natural frequency and power separately, to evaluate the electrical performance of the PANI/PVDF-TrFE bulk. When the oscillation frequency increased from 5 Hz to 30 Hz, the corresponding output voltage increased from 48 V to 246 V in Fig. 4a. As the frequency increases, the rate of change of the electric dipole moment in the bulk is accelerated, resulting in less charge escaped and more charge accumulated on both surfaces. Besides, due to the porosity of the bulk, there are many holes in the material that are prone to triboelectricity and static electricity, further increasing the potential difference between the two electrodes of the bulk [59]. As the applied pressure increased from 0.06 MPa to 0.31 MPa (Fig. S4), the corresponding output voltage of PTNG raised from 70 V to 246 V (Fig. 4b). Slightly different from the frequency change, as the power increases, the forward pressure on the bulk becomes larger, which in turn increases the amplitude of the electric dipole moment change, resulting in a higher potential. The response to frequency and power that the output voltage illustrates significant changes, which shows that it is sensitive and suitable for the preparation of pressure detection equipment that can be used in different frequency and stress environment.

To verify the role of PANI as carrier, PANI/PVDF-TrFE PTNGs with different pH and filling rate were prepared. The conductivity of PANI decreased with the increase of PH. It was conductivity at pH = 1–2, Semi conductivity at pH = 3–4 and insulation at pH = 5–6 [60]. For this reason, the output performance of the device under different acidic conditions was studied, of which open-circuit voltage is shown in Fig. 4c. With the increase of pH, the corresponding output voltage of PANI/PVDF-TrFE PTNG decreased from 246 V to 170 V, which proves that PANI has a positive impact on the electrical performance of the equipment. With the increase of PANI filling ratio, the output voltage of PTNG increased at first and then decreased, of the order of a maximum output voltage reached 246 V at 3 wt% in Fig. 4d. At low concentrations, as the content of PANI increases, the carrier density increases, which forms a good conductive network with PVDF-TrFE, thereby promoting charge transfer. As the filling rate further increases, PANI cannot fully diffuse and cause agglomeration (Fig. 3c and d), which seriously affects the electrical performance of the device. Under the same working environment, the output current of PTNGs with different pH and PANI

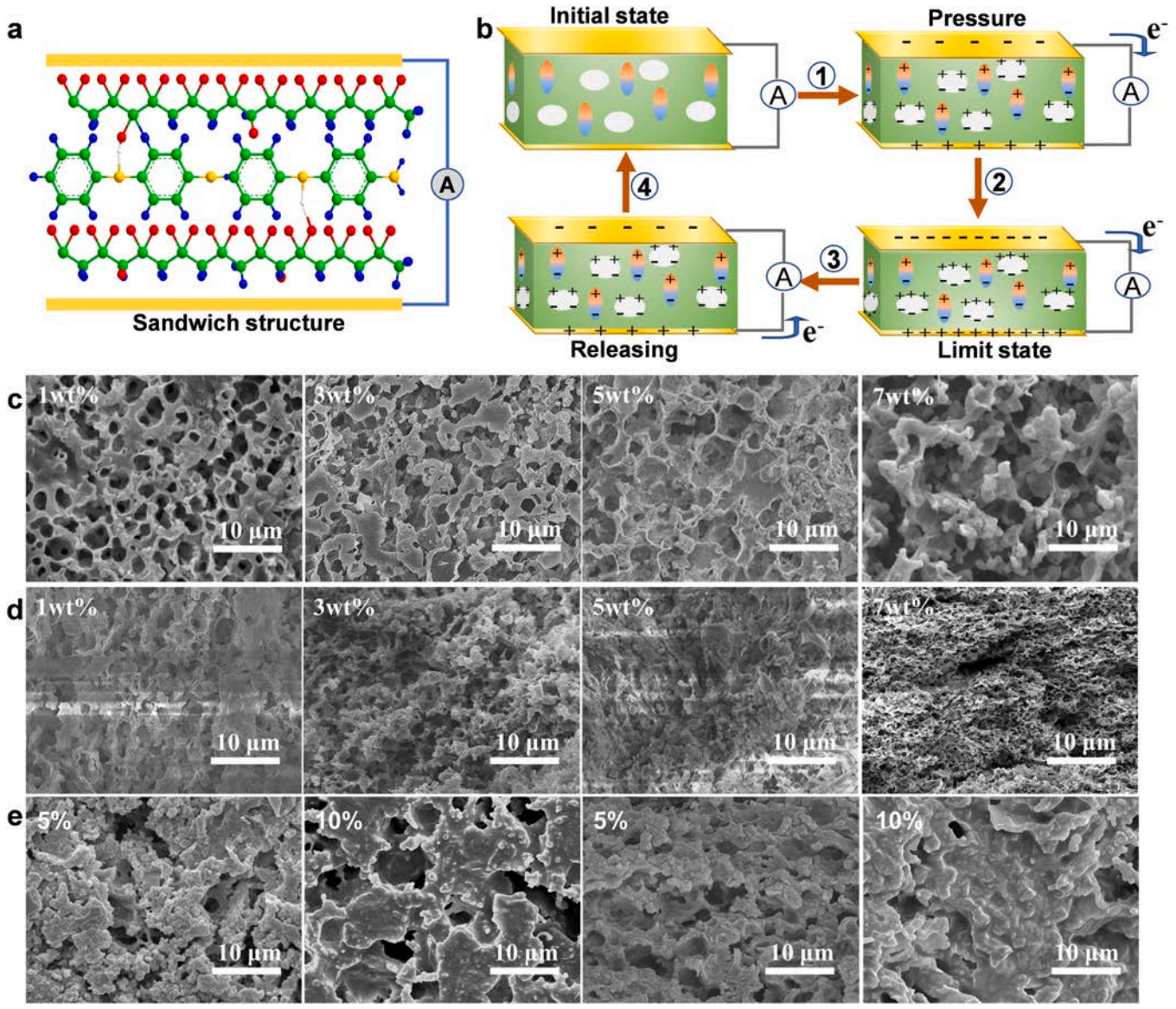

Fig. 3. (a) Conductive network between PANI and PVDF-TrFE through hydrogen bond and dipole interaction; (b) Structure and mechanism diagram of porous PANI/PVDF-TrFE bulks with periodic compressive force; (c) SEM images of the surface of PANI/PVDF-TrFE bulks filled with different PANI; (d) SEM images of the cross section of PANI/PVDF-TrFE bulks filled with different PANI; (e) SEM images of the surface and cross-section of PANI/PVDF-TrFE bulk infiltrated at 5% and 10% PDMS.

filling are shown in Fig. 4e. The PANI/PVDF-TrFE PTNG with pH of 1–2 and PANI filling rate of 3 wt% shows the best output performance, which reaches current of 122 μA.

Thickness is also an important factor affecting the output performance of the PTNG. Therefore, porous PANI/PVDF-TrFE bulks with thickness of 0.12 mm, 0.16 mm, 0.20 mm, 0.26 mm and 0.33 mm were prepared, and the corresponding output voltages were shown in Fig. 4f. When the thickness increased from 0.12 mm to 0.26 mm, the corresponding output voltage increased at first and then decreases, and the maximum output voltage reached 246 V when the thickness was 0.20 mm. This can be explained by the deformation. With the increase of the thickness of the bulk, under the same forward stress, extensive dipole moment compression can produce higher charge output as result of greater deformation of the bulk. When the thickness reached a certain value, the increase of internal resistance affected the charge transfer efficiency and led to the decrease of output performance. Compared with previous studies (Table S4), it is gratifying that the PANI/PVDF-TrFE PTNG exhibits excellent electrical output performance between 0.12 and 0.33 mm thickness, which indicates the possibility for the preparation of bulk nanogenerators with excellent electrical properties.

Compared with the uncleaned bulk, the ultrasonic-cleaned bulk exhibits a rich pore structure and smaller elastic modulus, and can achieve better electrical output performance in Figs. S3, S6 and 4g. To further analyze the effect of porosity on electrical properties, the prepared bulks were immersed in PDMS/xylene solutions with different concentrations to prepare PDMS/PANI/PVDF-TrFE bulks with different porosities. Among them, the concentrations of PDMS were 0%, 5%, and 10% respectively (Fig. 4h), and the pore structure was analyzed by Brunner-Emmet-Teller (BET) measurement. The corresponding information can be found in the Supporting information (Table S2 and Fig. S7). The voltage mainly depends on the synergy of the porosity and elastic modulus of the material [57]. When the PDMS concentration increase from 0% to 5%, the macropores and pore defects in the material are reduced in Fig. 3h, and the voids can be fully contacted under the action

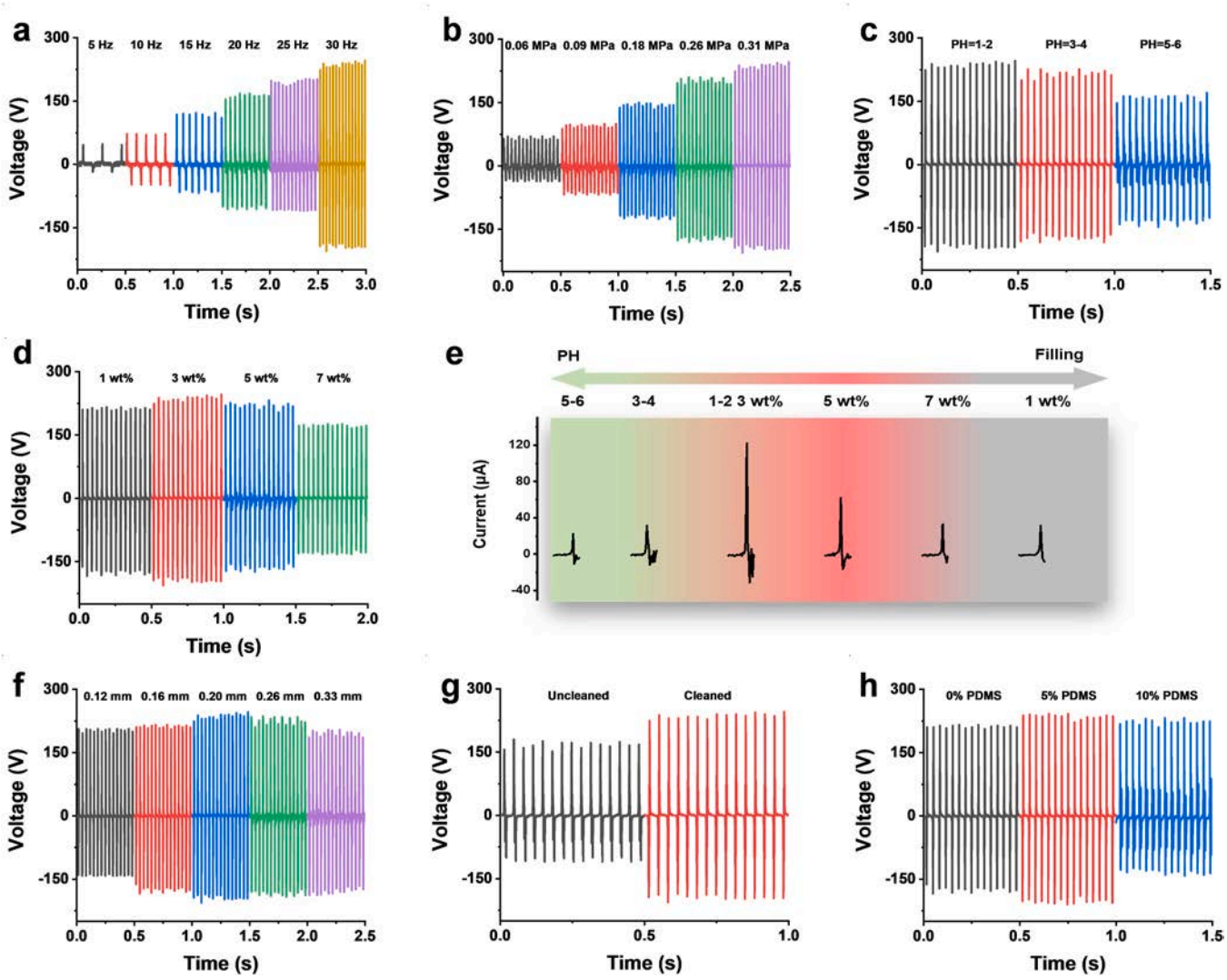

Fig. 4. (a) Response of PANI/PVDF-TrFE PTNG under different frequencies; (b) Response of PANI/PVDF-TrFE PTNG under different pressures; (c) Output voltage of PANI/PVDF-TrFE PTNGs prepared under different pH; (d) Output voltage of PANI/PVDF-TrFE PTNGs prepared under different PANI filling rates; (e) Output current of PANI/PVDF-TrFE PTNGs prepared under different pH and PANI filling rates; (f) Response of PTNGs under different thicknesses; (g) Output performance of PANI/PVDF-TrFE bulk before and after cleaning; (h) Response of PTNGs under different porosity.

of external force, thus generating and accumulating more charge on the surface. When the PDMS concentration increases from 5% to 10%, the pore size decreases and the specific surface area reaches saturation, which cannot hold more electric charge. At the same time, the increase of the elastic modulus of the material affects the piezoelectric effect, which leads to the decrease of the output voltage. According to the influence of the synergistic effect of pore size and porosity on PTNG, the concentration of PDMS can be controlled to reasonably adjust the density and size of pores, providing guidance for subsequent preparation of corresponding high-performance components.

rcid="RC57284">In order to test the load capacity of PTNG in practical applications, the output voltage, current and power density were monitored at the external load ranging from 100 Ω to 100 MΩ [61]. With the increase of resistance, the corresponding output voltage increases from 52 mV to 230 V, and the output current showed an opposite trend (Fig. 5b). At the external load of 10 MΩ, the PTNG generated the peak output power density of 6.69 W/m^2 (Fig. 5c). Compared with previous study of PTNGs as shown in Table S4, the PANI/PVDF-TrFE PTNG with excellent stability (Fig. S8) can achieve better output effect under similar conditions, which will make it show greater advantages in practical applications. To further verify its practical application ability, the device was connected to 119 blue light-emitting diodes with a size of 3 mm (Fig. 5d and e) and successfully lit them under the oscillation excitation of 30 Hz and 0.31 MPa (Fig. 5f), and the related parameters and videos were given in the support information (Table S3, Fig. S9 and Video 1). The bulk PANI/PVDF-TrFE PTNG has excellent electrical properties, and its preparation process is expected to be an ideal solution for the preparation of high-performance nano-generator components.

Supplementary material related to this article can be found online at doi:10.1016/j.nanoen.2020.105519.

4. Conclusion

In summary, this work has emerged as a new paradigm for rapid preparation of large-size β-PVDF aerogel bulk by rapid cooling of liquid nitrogen, which can be directly utilized for the mass production of high-performance PVDF-based NGs. The phase-changed bulk, with a β-phase of 71% after an effective phase transition, can be directly used to assemble PTNG, which greatly reduces the time cost of polarization and

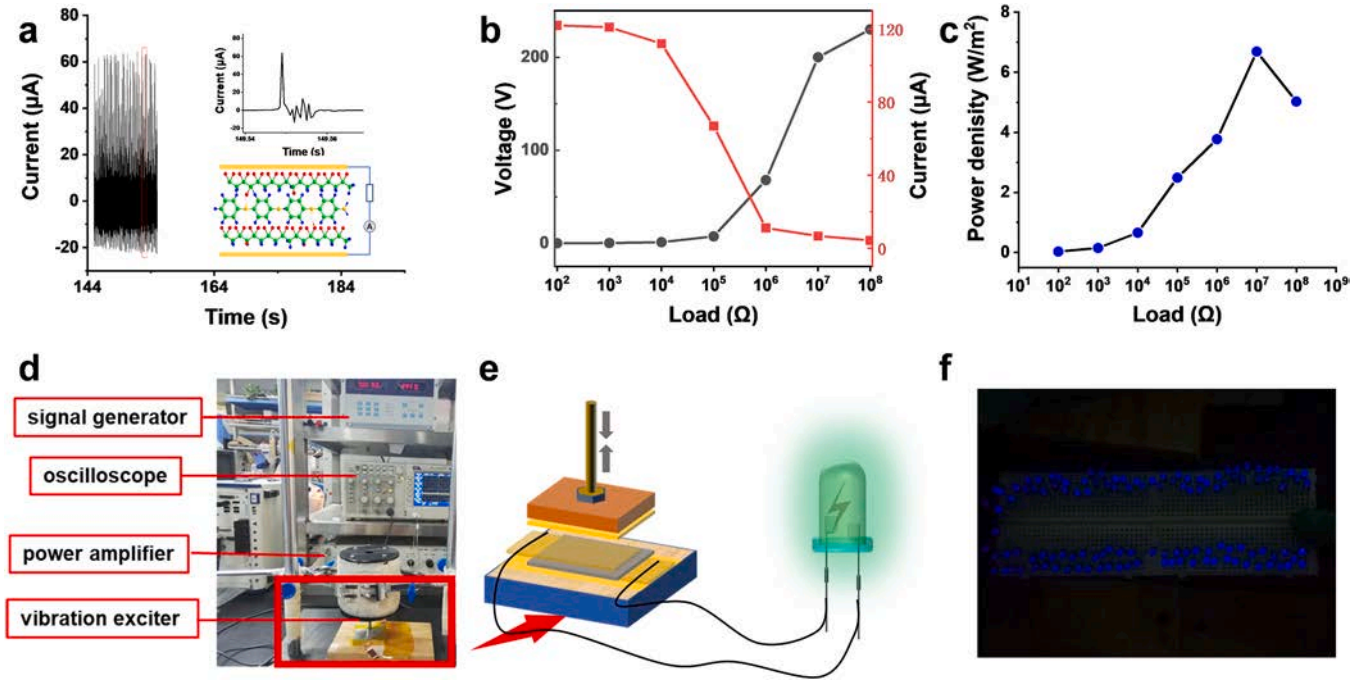

Fig. 5. (a) Output current of PANI/PVDF-TrFE PTNG under the external load of 100 kΩ; (b) The voltage and current density of the PANI/PVDF-TrFE PTNG with different resistances; (c) The load power density with different resistance; (d) The experimental testing platform; (e) Connection diagram of PANI/PVDF-TrFE PTNG and 119 LED bulbs; (f) The LED bulbs connected in series are illuminated by PANI/PVDF-TrFE PTNG.

shows feasibility for its industrial production. Besides, the pore structure caused by SCMC and the conductive network formed by PANI further promote the electrical property of the device. The effects of porosity, pH, filling rate, frequency, and force on device performance were researched. The fabricated PANI/PVDF-TrFE PTNG exhibited is capable of delivering a maximum output voltage of 246 V, output current of 122 μA, which corresponded to the power density of 6.69 W/m^2. Further, the efficient device can light up 119 blue light-emitting diodes in series with a size of 3 mm. Eliminating the need for subsequent polarization, PANI/PVDF-TrFE porous aerogel prepared here exhibits larger volume and higher β-phase concentration, with lower cost and shorter preparation cycle. There is reason to believe that this innovative method for rapid mass production of solid β-PVDF piezoelectric materials will undoubtedly show promising potential in the industrialization of high-performance PENG devices.

CRediT authorship contribution statement

Shengrui Yu: prepared and revised the manuscript; provided funding acquisition. **Yongkang Zhang:** performed the experiments; performed electrical properties testing; contributed to the performance investigation of the devices; prepared and revised the manuscript. **Zhaohan Yu:** conceived and designed the experiments; designed the mold and fabricated the devices; performed theoretical analysis; prepared and revised the manuscript. **Jiaqi Zheng:** fabricated the devices; contributed to the device fabrication. **Yunming Wang:** proposed the new strategy and supervised the whole project; conceived and designed the experiments; performed theoretical analysis; provided funding acquisition. **Huamin Zhou:** provided technical assistance and equipment; provided funding acquisition.

Declaration of Competing Interest

The authors declare that they have no known competing financial interests or personal relationships that could have appeared to influence the work reported in this paper.

Acknowledgments

This work was supported by the National Key Research and Development Program of China (Grant No. 2018YFB1106700), Double First-Class-Independent Innovation-Subject Construction (5001110032), General Program of National Natural Science Foundation of China (52075196), and the National Natural Science Foundation Council of China (Grant No. 51741505), the Natural Science Foundation of Jiangxi Province, China (No. 20202BABL204038), the Science and Technology Foundation of Jiangxi Educational Committee (No. GJJ180701), and the State Key Laboratory of Materials Processing and Die & Mould Technology, Huazhong University of Science and Technology (No. P2018-015).

Appendix A. Supporting information

Supplementary data associated with this article can be found in the online version at doi:10.1016/j.nanoen.2020.105519.

References

[1] C. Ribeiro, C.M. Costa, D.M. Correia, J. Nunes-Pereira, J. Oliveira, P. Martins, R. Goncalves, V.F. Cardoso, S. Lanceros-Mendez, Electroactive poly(vinylidene fluoride)-based structures for advanced applications, Nat. Protoc. 13 (2018) 681–704.
[2] Y. Han, C. Jiang, H. Lin, C. Luo, R. Qi, H. Peng, Piezoelectric nanogenerators based on helical carbon materials and polyvinyledenedifluoride–trifluoroethylene hybrids with enhanced energy-harvesting performance, Energy Technol. 8 (2020) 1901249.
[3] M. Khalifa, A. Mahendran, S. Anandhan, Durable, efficient, and flexible piezoelectric nanogenerator from electrospun PANi/HNT/PVDF blend nanocomposite, Polym. Compos. 40 (2019) 1663–1675.
[4] L. Jin, B. Zhang, L. Zhang, W. Yang, Nanogenerator as new energy technology for self-powered intelligent transportation system, Nano Energy 66 (2019), 104086.
[5] X. Guan, B. Xu, J. Gong, Hierarchically architected polydopamine modified BaTiO3@P(VDF-TrFE) nanocomposite fiber mats for flexible piezoelectric nanogenerators and self-powered sensors, Nano Energy 70 (2020), 104516.
[6] S.-J. Park, S. Lee, M.-L. Seol, S.-B. Jeon, H. Bae, D. Kim, G.-H. Cho, Y.-K. Choi, Self-sustainable wind speed sensor system with omni-directional wind based triboelectric generator, Nano Energy 55 (2019) 115–122.

[7] J. Zhu, X. Hou, X. Niu, X. Guo, J. Zhang, J. He, T. Guo, X. Chou, C. Xue, W. Zhang, The d-arched piezoelectric-triboelectric hybrid nanogenerator as a self-powered vibration sensor, Sens. Actuators A Phys. 263 (2017) 317–325.

[8] R.A. Surmenev, T. Orlova, A.A.I. Roman, V. Chernozema, A. Bartasyte, S. Mathur, M.A. Surmeneva, Hybrid lead-free polymer-based nanocomposites with improved piezoelectric response for biomedical energy-harvesting applications: a review, Nano Energy 62 (2019) 475–506.

[9] Z. Xu, C. Jin, A. Cabe, D. Escobedo, N. Hao, I. Trase, A.B. Closson, L. Dong, Y. Nie, J. Elliott, M.D. Feldman, Z. Chen, J.X.J. Zhang, Flexible energy harvester on a pacemaker lead using multibeam piezoelectric composite thin films, ACS Appl. Mater. Interfaces 12 (2020) 34170–34179.

[10] T. Yang, H. Pan, G. Tian, B. Zhang, D. Xiong, Y. Gao, C. Yan, X. Chu, N. Chen, S. Zhong, L. Zhang, W. Deng, W. Yang, Hierarchically structured PVDF/ZnO core-shell nanofibers for self-powered physiological monitoring electronics, Nano Energy 72 (2020), 104706.

[11] F. Mokhtari, Z. Cheng, R. Raad, J. Xi, J. Foroughi, Piezofibers to smart textiles: a review on recent advances and future outlook for wearable technology, J. Mater. Chem. A 8 (2020) 9496–9522.

[12] Q. Zhang, Z. Zhang, Q. Liang, F. Gao, F. Yi, M. Ma, Q. Liao, Z. Kang, Y. Zhang, Green hybrid power system based on triboelectric nanogenerator for wearable/portable electronics, Nano Energy 55 (2019) 151–163.

[13] X. Mo, H. Zhou, W. Li, Z. Xu, J. Duan, L. Huang, B. Hu, J. Zhou, Piezoelectrets for wearable energy harvesters and sensors, Nano Energy 65 (2019), 104033.

[14] B. Mahanty, K. Maity, S. Sarkar, D. Mandal, Mater. Today Proc. 21 (2020) 1964–1968.

[15] K. Maity, S. Garain, K. Henkel, D. Schmeißer, D. Mandal, Self-powered human-health monitoring through aligned PVDF nanofibers interfaced skin-interactive piezoelectric sensor, ACS Appl. Polym. Mater. 2 (2020) 862–878.

[16] S. Sutradhar, S. Saha, S. Javed, Shielding effectiveness study of barium hexaferrite-incorporated, β-phase-improved poly(vinylidene fluoride) composite film: a metamaterial useful for the reduction of electromagnetic pollution, ACS Appl. Mater. Interfaces 11 (2019) 23701–23713.

[17] N. Hussain, M.H. Zhang, Q. Zhang, Z. Zhou, X. Xu, M. Murtaza, R. Zhang, H. Wei, G. Ou, D. Wang, K. Wang, J.F. Li, H. Wu, Large piezoelectric strain in sub-10 nanometer two-dimensional polyvinylidene fluoride nanoflakes, ACS Nano 13 (2019) 4496–4506.

[18] S. Qin, X. Zhang, Z. Yu, F. Zhao, Polarization study of poly(vinylidene fluoride) films under cyclic electric fields, Polym. Eng. Sci. 60 (2020) 645–656.

[19] A. Ferri, S. Barrau, R. Bourez, A. Da Costa, M.H. Chambrier, A. Marin, J. Defebvin, J.M. Lefebvre, R. Desfeux, Probing the local piezoelectric behavior in stretched barium titanate/poly(vinylidene fluoride) nanocomposites, Compos. Sci. Technol. 186 (2020), 107914.

[20] L.L. Sun, B. Li, Z.G. Zhang, W.H. Zhong, Achieving very high fraction of β-crystal PVDF and PVDF/CNF composites and their effect on AC conductivity and microstructure through a stretching process, Eur. Polym. J. 46 (2010) 2112–2119.

[21] J. Wang, H. Li, J. Liu, Y. Duan, S. Jiang, S. Yan, On the α → β transition of carbon-coated highly oriented PVDF ultrathin film induced by melt recrystallization, J. Am. Chem. Soc. 125 (2003) 1496–1497.

[22] H. Guo, J. Li, Y. Meng, J. de Claville Christiansen, D. Yu, Z. Wu, S. Jiang, Stretch-induced stable-metastable crystal transformation of PVDF/graphene composites, Polym. Cryst. 2 (2019), e10079.

[23] Z. Guan, H. Hu, X. Shen, P. Xiang, N. Zhong, J. Chu, C. Duan, Recent progress in two-dimensional ferroelectric materials, Adv. Electron. Mater. 6 (2020) 1900818.

[24] C. Cui, F. Xue, W.-J. Hu, L.-J. Li, Two-dimensional materials with piezoelectric and ferroelectric functionalities, npj 2D Mater. Appl. 2 (2018) 18.

[25] P. Martins, A.C. Lopes, S. Lanceros-Mendez, Electroactive phases of poly (vinylidene fluoride): determination, processing and applications, Prog. Polym. Sci. 39 (2014) 683–706.

[26] A. De Neef, C. Samuel, G. Stoclet, M. Rguiti, C. Courtois, P. Dubois, J. Soulestin, J. M. Raquez, Processing of PVDF-based electroactive/ferroelectric films: importance of PMMA and cooling rate from the melt state on the crystallization of PVDF beta-crystals, Soft Matter 14 (2018) 4591–4602.

[27] Y. Park, Y.-E. Shin, J. Park, Y. Lee, M.P. Kim, Y.-R. Kim, S. Na, S.K. Ghosh, H. Ko, Ferroelectric multilayer nanocomposites with polarization and stress concentration structures for enhanced triboelectric performances, ACS Nano 14 (2020) 7101–7110.

[28] F. Calavalle, M. Zaccaria, G. Selleri, T. Cramer, D. Fabiani, B. Fraboni, Piezoelectric and electrostatic properties of electrospun PVDF-TrFE nanofibers and their role in electromechanical transduction in nanogenerators and strain sensors, Macromol. Mater. Eng. 305 (2020) 2000162.

[29] X. Mei, L. Lu, Y. Xie, W. Wang, Y. Tang, K.S. Teh, An ultra-thin carbon-fabric/graphene/poly(vinylidene fluoride) film for enhanced electromagnetic interference shielding, Nanoscale 11 (2019) 13587–13599.

[30] H. Zhang, Y. Zhu, L. Li, Fabrication of PVDF/graphene composites with enhanced β phaseviaconventional melt processing assisted by solid state shear milling technology, RSC Adv. 10 (2020) 3391–3401.

[31] M.H. Syu, Y.J. Guan, W.C. Lo, Y.K. Fuh, Biomimetic and porous nanofiber-based hybrid sensor for multifunctional pressure sensing and human gesture identification via deep learning method, Nano Energy 76 (2020), 105029.

[32] Q. Zheng, L. Fang, H. Guo, K. Yang, Z. Cai, M.A.B. Meador, S. Gong, Highly porous polymer aerogel film-based triboelectric nanogenerators, Adv. Funct. Mater. 28 (2018) 1706365.

[33] Y. Tang, Q. Zheng, B. Chen, Z. Ma, S. Gong, A new class of flexible nanogenerators consisting of porous aerogel films driven by mechanoradicals, Nano Energy 38 (2017) 401–411.

[34] K. Xia, Z. Zhu, H. Zhang, C. Du, Z. Xu, R. Wang, Painting a high-output triboelectric nanogenerator on paper for harvesting energy from human body motion, Nano Energy 50 (2018) 571–580.

[35] K. Xia, D. Wu, J. Fu, Z. Xu, A pulse controllable voltage source based on triboelectric nanogenerator, Nano Energy 77 (2020), 105112.

[36] K. Xia, J. Fu, Z. Xu, Multiple-frequency high-output triboelectric nanogenerator based on a water balloon for all-weather water wave energy harvesting, Adv. Energy Mater. 10 (2020) 2000426.

[37] S. Gupta, R. Bhunia, B. Fatma, D. Maurya, D. Singh, Prateek R. Gupta, S. Priya, R. K. Gupta, A. Gar, Multifunctional and flexible polymeric nanocomposite films with improved ferroelectric and piezoelectric properties for energy generation devices, ACS Appl. Energy Mater. 2 (2019) 6364–6374.

[38] H. Luo, X. Zhou, C. Ellingford, Y. Zhang, S. Chen, K. Zhou, D. Zhang, C.R. Bowen, C. Wan, Interface design for high energy density polymer nanocomposites, Chem. Soc. Rev. 48 (2019) 4424–4465.

[39] R. Lin, A. Li, L. Lu, Y. Cao, Preparation of bulk sodium carboxymethyl cellulose aerogels with tunable morphology, Carbohydr. Polym. 118 (2015) 126–132.

[40] S. Biswas, B. Dutta, S. Bhattacharya, Correlation between nucleation, phase transition and dynamic melt-crystallization kinetics in PAni/PVDF blends, RSC Adv. 5 (2015) 74486–74498.

[41] P. Yang, D. Lv, W. Shen, T. Wu, Y. Yang, Y. Zhao, R. Tan, W. Song, Porous flexible polyaniline/polyvinylidene fluoride composite film for trace-level NH3 detection at room temperature, Mater. Lett. 271 (2020), 127798.

[42] W. Liao, H.-B. Zhao, Z. Liu, S. Xu, Y.-Z. Wang, On controlling aerogel microstructure by freeze casting, Compos. Part B Eng. 173 (2019), 107036.

[43] L. Jie, L. Zheng, Interaction between 1-dodecyl-3-methylimidazolium bromide and sodium carboxymethylcellulose in aqueous solution: effect of polymer concentration, J. Dispers. Sci. Technol. 33 (2012) 5–14.

[44] V. Gautam, K.P. Singh, V.L. Yadav, Preparation and characterization of green-nano-composite material based on polyaniline, multiwalled carbon nano tubes and carboxymethyl cellulose: for electrochemical sensor applications, Carbohydr. Polym. 189 (2018) 218–228.

[45] Y. Liu, L. Xie, W. Zhang, Z. Dai, W. Wei, S. Luo, X. Chen, W. Chen, F. Rao, L. Wang, Y. Huang, Conjugated system of PEDOT:PSS-induced self-doped PANI for flexible zinc-ion batteries with enhanced capacity and cyclability, ACS Appl. Mater. Interfaces 11 (2019) 30943–30952.

[46] D. Punetha, M. Kar, S.K. Pandey, A new type low-cost, flexible and wearable tertiary nanocomposite sensor for room temperature hydrogen gas sensing, Sci. Rep. 10 (2020) 2151.

[47] X. Cai, T. Lei, D. Sun, L. Lin, A critical analysis of the α, β and γ phases in poly (vinylidene fluoride) using FTIR, RSC Adv. 7 (2017) 15382–15389.

[48] L.T. Cuba-Chiem, L. Huynh, J. Ralston, D.A. Beattie, In situ particle film ATR FTIR spectroscopy of carboxymethyl cellulose adsorption on talc: binding mechanism, pH effects, and adsorption kinetics, Langmuir 24 (2008) 8036–8044.

[49] N. Meng, X. Ren, G. Santagiuliana, L. Ventura, H. Zhang, J. Wu, H. Yan, M.J. Reece, E. Bilotti, Ultrahigh β-phase content poly(vinylidene fluoride) with relaxor-like ferroelectricity for high energy density capacitors, Nat. Commun. 10 (2019) 4535.

[50] F. Chen, Y. Wu, Z. Ding, X. Xia, S. Li, H. Zheng, C. Diao, G. Yue, Y. Zi, A novel triboelectric nanogenerator based on electrospun polyvinylidene fluoride nanofibers for effective acoustic energy harvesting and self-powered multifunctional sensing, Nano Energy 56 (2019) 241–251.

[51] D. Sohn, J.W. Ko, E.J. Son, S.H. Ko, T.-H. Kim, H. Kwon, C.B. Park, Cellulose-templated, dual-carbonized Na3V2(PO4)3 for energy storage with high rate capability, ChemElectroChem 5 (2018) 2186–2191.

[52] P. Yadav, T.D. Raju, S. Badhulika, Self-poled hBN-PVDF nanofiber mat-based low-cost, ultrahigh-performance piezoelectric nanogenerator for biomechanical energy harvesting, ACS Appl. Electron. Mater. 2 (2020) 1970–1980.

[53] I. Kim, H. Roh, J. Yu, N. Jayababu, D. Kim, Boron nitride nanotube-based contact electrification-assisted piezoelectric nanogenerator as a kinematic sensor for detecting the flexion–extension motion of a robot finger, ACS Energy Lett. 5 (2020) 1577–1585.

[54] X. Ma, S. Li, S. Dong, J. Nie, M. Iwamoto, S. Lin, L. Zheng, X. Chen, Regulating the output performance of triboelectric nanogenerator by using P(VDF-TrFE) Langmuir monolayers, Nano Energy 66 (2019), 104090.

[55] C. Xu, B. Zhang, A.C. Wang, H. Zou, G. Liu, W. Ding, C. Wu, M. Ma, P. Feng, Z. Lin, Z.L. Wang, ACS Nano 13 (2019) 2034–2041.

[56] F.-R. Fan, Z.-Q. Tian, Z. Lin Wang, Flexible triboelectric generator, Nano Energy 1 (2012) 328–334.

[57] Q. Zheng, H. Zhang, H. Mi, Z. Cai, Z. Ma, S. Gong, High-performance flexible piezoelectric nanogenerators consisting of porous cellulose nanofibril (CNF)/poly (dimethylsiloxane) (PDMS) aerogel films, Nano Energy 26 (2016) 504–512.

[58] X. Wang, B. Yang, J. Liu, C. Yang, A transparent and biocompatible single-friction-surface triboelectric and piezoelectric generator and body movement sensor, J. Mater. Chem. A 5 (2017) 1176–1183.

[59] K. Shi, X. Huang, B. Sun, Z. Wu, J. He, P. Jiang, Cellulose/BaTiO3 aerogel paper based flexible piezoelectric nanogenerators and the electric coupling with triboelectricity, Nano Energy 57 (2019) 450–458.

[60] S.J. Kim, S.R. Shin, G.M. Spinks, I.Y. Kim, S.I. Kim, Synthesis and characteristics of a semi-interpenetrating polymer network based on chitosan/polyaniline under different pH conditions, J. Appl. Polym. Sci. 96 (2005) 867–873.

[61] Z. Yu, Y. Wang, J. Zheng, Y. Xiang, P. Zhao, J. Cui, H. Zhou, D. Li, Rapidly fabricated triboelectric nanogenerator employing insoluble and infusible biomass materials by fused deposition modeling, Nano Energy 68 (2020), 104382.

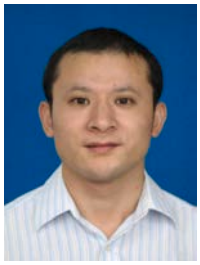

Shengrui Yu received his Ph.D. degree from Huazhong University of Science and Technology in 2014. He is currently an associate professor in the School of Mechanical and Electronic Engineering at Jingdezhen Ceramic Institute. His research mainly focuses on triboelectric and piezoelectric nanogenerator, advanced polymer processing technology and equipment, and novel methods for polymer processing.

Yongkang Zhang received his bachelor degree in School of Mechanical and Electronic Engineering, Jingdezhen Ceramic Institute in 2018. He is currently a master student in the School of Mechanical and Electronic Engineering, Jingdezhen Ceramic Institute, Jingdezhen, P.R. China, under the supervision of associate professor Shengrui Yu. His master's research interests include experimental and theoretical research: piezoelectric polymer material, piezoelectric and triboelectric nanogenerators.

Zhaohan Yu received her bachelor degree in Materials Science and Engineering at Huazhong University of Science and Technology in 2017. She is currently a Ph.D. student in the School of Materials Science and Engineering at the Huazhong University of Science and Technology, Wuhan, P.R. China, under the supervision of professor Dequn Li. Her PhD's research interests include experimental and theoretical research: piezoelectric and triboelectric nanogenerators, biomass materials and 3D printing.

Jiaqi Zheng received her bachelor degree in School of Materials Science and Engineering at the Huazhong University of Science and Technology in 2019. She is currently a M.S. candidate in the School of Materials Science and Engineering at the Huazhong University of Science and Technology. Her undergraduate research interests include preparation of nanostructures and piezoelectric nanogenerators.

Yunming Wang received his Ph.D. degree from Dalian University of Technology in 2013. He is currently an associate professor in the School of Materials Science and Technology at Huazhong University of Science and Technology. His research interests include multifunctional nanocomposites, triboelectric and piezoelectric nanogenerator, 3D printing and electronic skin.

Huamin Zhou received his B.S. and Ph.D. degree from Huazhong University of Science and Technology in 1996 and 2001, respectively. He is currently a professor and the dean of the School of Materials Science and Engineering. His research interests include materials science, numerical modeling/simulation and novel methods for polymer processing.